Catalysis of the Oxygen Reduction Reaction on Bimetallic PtCu Nanostructures

Eric Coleman and Anne Co

Chemistry and Biochemistry, The Ohio State University, Columbus, OH 42310, USA

Abstract: We describe the design and synthesis of Pt-Cu electrocatalysts with well-defined, tunable morphology and composition. Electron microscopy and Brunauer-Emmett-Teller (BET) surface analysis indicate our catalysts have extremely high porosity, which acts to maximize mass transport, increase active surface area, and minimize the overall precious metal content. Production of these catalysts is quite facile and begins with synthesis of a porous Cu substrate, formed by etching Al from a Cu-Al alloy. The porous Cu substrate is then coated with a Pt layer via galvanic replacement with K_2PtCl_4. Growth of the Pt layer is manipulated by time, temperature, concentration of K_2PtCl_4, and convection rate during galvanic replacement. Data from inductively coupled plasma-mass spectrometry (ICP-MS) and energy dispersive X-ray spectroscopy (EDX) confirm multiple Pt loadings have been achieved via the galvanic replacement process. The Pt layer was found to enhance the oxygen reduction activity 30%-75% relative to the current state-of-the-art Pt/C catalyst and act as a barrier towards corrosion of the Cu understructure. The high ORR activity obtained indicates that high catalytic activity could potentially be achieved from fine-tuning this technique for other bimetallic Pt-based catalysts.

1. Introduction

Proton exchange membrane fuel cells (PEMFCs) are electrochemical energy conversion devices which exploit the favorable energetics of the reaction between molecular hydrogen and oxygen to produce water. PEMFCs have attracted substantial attention due to their high conversion efficiency, high energy density, and low carbon footprint. These devices offer the promise of energy production for applications ranging from portable electronics to the transportation

sector.[1-2] However, PEMFCs are not widely commercialized primarily because of the slow kinetics of the oxygen reduction reaction (ORR) occurring at the cathode.[3] Pt and Pt-based materials remain the best catalysts for catalyzing the ORR, but still do not fully compensate for their expense with their performance.[3-5] Before fuel cells can become economically viable, efforts must be taken to decrease Pt content while maintaining a high level of ORR activity.[6-7] In recent years, much research and theory has been dedicated to developing bimetallic catalyst systems where Pt is alloyed with 3d block metals, usually Fe, Ni, Co or Cu.[5, 8-20] These catalysts have lower Pt loadings and increased activity relative to bulk Pt, mainly due to geometric and electronic effects.[10, 21-22] There are many approaches to preparing these catalysts, but most involve a.) preparing Pt-X (X = Fe, Ni, Co, or Cu) catalyst nanoparticles[14, 23-28] or b.) preparing core-shell (core = Ni, Co, Cu or PtX; shell = Pt) catalysts.[9, 16, 22-23, 29-40] If the layer of Pt on the surface of core-shell catalysts is $\leq$ 1 nm thick (usually via electrochemical dealloying), experiment and theory shows there is a fourfold increase in ORR activity due to introduction of lattice strain to the Pt shell.[29] While these bimetallic methods have all proven to significantly enhance the ORR, they possess certain intrinsic shortcomings. First, any catalyst designs relying upon nanoparticles are susceptible to activity losses due to particle growth by Ostwald ripening.[11] Second, core-shell and nanoparticle catalyst designs usually require very intensive synthesis processes and/or temperatures exceeding 800 °C[19, 33-35]—neither of which are ideal for industrial scale catalyst production. An optimal Pt-based ORR catalyst should incorporate all the benefits of these proven bimetallic catalyst designs but remain electrically connected and involve a facile synthesis. Recently, galvanic displacement or transmetallization has emerged as a powerful yet facile route to the development of highly active Pt-based bimetallic ORR catalysts.[16-17, 32, 38-42] However, galvanic displacement is usually coupled with nanoparticle

synthesis,[16, 23, 41] which again, can be quite complex. We employed galvanic displacement to coat thin layers of Pt on three dimensional nanoporous Cu foams to produce highly active and stable core-shell ORR catalysts. There are several advantages to this method: 1) catalysts remain electrically connected because they are supported on a continuous metal substrate, 2) catalysts maintain a high surface area—the porous nanostructure offers a similar catalytic enhancement to nanoparticles, 3) oxygen is able to freely diffuse into pores, increasing overall catalyst utilization, 4) particle growth from Ostwald ripening is eliminated, and 5) catalyst synthesis is facile and can easily be brought to industrial scale. To the best of our knowledge, we are the first to report a catalyst of this type being used for the ORR. A similar catalyst was designed by Xu et al.,[40] but used for methanol oxidation. While the benefits of this core-shell catalyst design are plentiful, electrochemical half-cell testing of metal foams is not trivial. Nanostructured materials like this have poorly understood rotating disk electrode (RDE) profiles, and with the exception of membrane electrode assembly (MEA) tests, there is no universally accepted standard for testing the ORR. Since we do not currently have the MEA capability, we used the widely-accepted thin-layer RDE approach[3] for preliminary electrochemical characterization of our catalysts.

Most thin-layer RDE testing requires that the fully functional catalyst, as prepared, be drop cast onto a glassy carbon (GC) electrode. Our methodology is novel, because we drop cast our nanostructured Cu onto a GC RDE electrode, allow it to dry, and then perform galvanic displacement (under rotation control) to complete the catalyst synthesis. This method is beneficial because it 1) allows for fine-tuning of the galvanic displacement process and 2) decreases the synthesis time, as there is no need for successive washing/centrifugation to isolate the catalyst particles. Using this procedure, we discovered that by manipulating several parameters (i.e. time/temperature) during the galvanic displacement process we could vary the

ORR activity. This work provides a comprehensive look at ORR activity as a function of those parameters, and seeks to justify some of the changes in activity with specific morphological changes occurring on the catalysts.

2. Experimental

Nanoporous (NP) copper synthesis

A 70% aluminum 30% copper (at %) alloy was prepared from bulk metals using a foundry. The alloy was cut into 24 mm x 2 mm 'coins'. To etch Al and achieve the nanoporous Cu structure, a coin was immersed in 100 mL of a 6 M NaOH solution and the solution heated to 80 °C and aged for 16 hours under magnetic stirring. The Cu coin was then removed from the solution and immersed in 1 L of ultrapure water (Milli-Q 18.2 MΩ resistivity). After 2 hours the water was exchanged to ensure complete removal of byproducts from the etching process. To reduce all copper species to a zero oxidation state the coin was calcined in a tube furnace for 2 hours at 450 °C in H_2. Following calcination, the reduced copper coin was ground into a fine powder using a mortar and pestle. NP Cu powder was stored in vacuum sealed bags. The morphology of NP Cu after preparation is shown in Figure 1.

Thin-layer NP Cu electrode preparation

a.) Unsupported catalysts: 15 mg NP Cu powder was dispersed ultrasonically in 10 mL of ultrapure H_2O for 10 minutes. 40 μL of a diluted Nafion® solution (5 wt % Alfa Aesar) was added to the NP Cu dispersion. The resulting solution was sonicated for another 10 min. Immediately following sonication, 20 μL of the suspension was drop-cast onto a polished glassy carbon (GC) disk electrode (Pine, 5 mm diameter). The prepared electrode was dried under vacuum at ~55 °C for 1.5 hours. After drying, the coated electrode was allowed to cool down to room temperature.

b.) Carbon supported catalysts: 7.5 mg NP Cu powder and 7.5 mg carbon (Vulcan XC-72) was dispersed ultrasonically in 10 mL of ultrapure H_2O for 10 minutes. There were no other variations from the prior procedure.

c.) For comparison, 20 wt % Pt Black supported on carbon (Vulcan XC-72) was prepared by dispersing 3.0 mg Pt Black (Alfa Aesar) and 12.0 mg Vulcan XC-72 in 10 mL of ultrapure H_20 for 10 minutes. There were no other variations from the prior procedure.

Deposition of platinum

120 mL of a 1.2 mM or 0.12 mM K_2PtCl_4 (Sigma-Aldrich) solution (ultrapure H_2O) was added to a standard 3-electrode cell with heating jacket. Depending on the deposition, the cell was thermostated between 40 and 60 °C. The copper coated GC electrode was attached to a Pine electrode rotator and immersed in the K_2PtCl_4 solution for 1-40 minutes. To ensure uniform deposition of platinum, the electrode was rotated at 500 rpm. Immediately after the timed deposition, the electrode was removed from the platinum solution and rinsed in 200 mL of ultrapure water for 2 minutes (500 rpm).

Electrochemical measurements

Electrochemical measurements were performed in a jacketed standard 3-electrode cell using a ring-disk electrode (Pine) with a bi-potentiostat (Pine WaveDriver) under rotation control. A reversible hydrogen electrode (RHE) was the reference electrode for all electrochemical measurements. The counter electrode was a Pt mesh. The electrolyte used was 0.1 M $HClO_4$, which was prepared by diluting concentrated trace metal grade acid (Fisher) with ultrapure H_2O. All cyclic voltammograms were recorded at 298K with a scan rate of 100 mV s^{-1} and a rotation rate of 1600 rpm. The prepared electrodes were transferred to the electrochemical cell and immersed in nitrogen-saturated electrolyte. The electrodes were 'primed' via electrochemical dealloying using a modification of the method first described by Koh et al.[43] The potential was

cycled 50 times between 0.5 V and 1.2 V to dealloy/stabilize the catalyst. Then CV scans 0 V-1.2 V were obtained until multiple stable voltammograms were recorded. The Pt electrochemical surface area (Pt-ECSA) was determined from a stable N_2 saturated voltammogram via the average integrated charge of the underpotentially deposited hydrogen (H_{upd}) region (0.05 V to 0.40) after double-layer correction. The widely accepted conversion of 210 μC cm^{-2}_{Pt} for polycrystalline Pt was assumed.[44] ORR CV measurements were performed in oxygen-saturated electrolyte with the potential cycled between 0.0 V and 1.2 V. Kinetic ORR activity was calculated for the *anodic sweep* via the following relationship:

$$i_k = \frac{i_{lim}\, i_{tot}}{i_{lim} - i_{tot}}$$

Pt specific activities were determined from Pt-ECSA data as follows:

$$i_{Pt} = \frac{i_k}{Pt\ ECA}$$

Electrochemical impedance spectroscopy (EIS) was used to determine the solution resistance for the electrochemical system to correct all data for IR loss. A Princeton Applied Research 263A potentiostat was used in conjunction with a Solartron 1260 Impedance Analyzer. The impedance was measured at 0.9 V (amplitude of 5 mV from 10,000 Hz to 0.01 Hz). The correction was applied to raw data as follows:

$$E_{real} = E_{measured} - E_{IR}$$

Catalyst physical characterization

Mass and loading measurements were performed on a Perkin-Elmer Sciex Elan 6000 ICP-MS using catalyst-coated GC electrodes dissolved in aqua regia (3 HCl:1 HNO_3). Morphology of the catalysts was studied using a scanning electron microscope (SEM) (FEI Sirion XL 30) with an energy dispersive X-ray (EDX) detector.

3. Results and Discussion

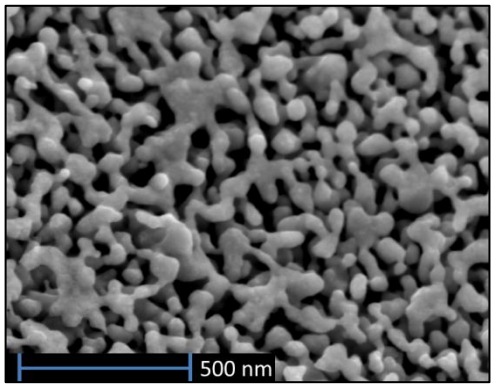

Figure 1. SEM image of NP Cu after dealloying Al from Cu-Al alloy with 6 M NaOH.

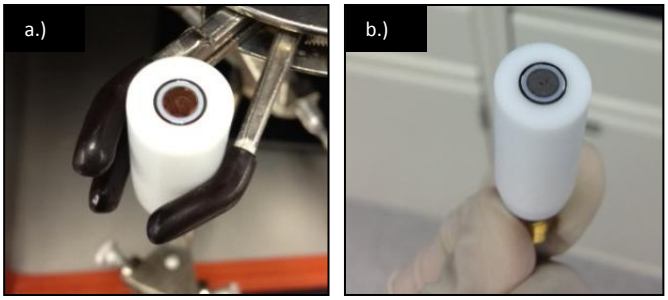

Figure 2. Images of glassy carbon disk electrode with a.) NP Cu w/ Nafion and b.) PtCu catalyst after 5 min galvanic displacement at room temperature w/ 1.2 mM K_2PtCl_4.

Figure 1 shows NP Cu prepared by dealloying Al from a Cu-Al alloy (65% Al) in 6 M NaOH for 16 hours. The porous structure is quite uniform with an average ligament size of ~ 60 nm. BET measurements give an average surface area of 13 $m^2\ g^{-1}$. The ligament size, porosity, and surface area can be tuned by varying a.) the % composition of the Cu-Al alloy, b.) the pouring temperature of the Cu-Al alloy, c.) the NaOH concentration, and d.) the subsequent reduction/annealing temperature.

The galvanic displacement process is driven by the difference in standard reduction potentials of the $Pt/PtCl_4^{2-}$ redox couple ($E^0 = 0.730\ V_{SHE}$) and the Cu/Cu^{2+} redox couple ($E^0 = 0.341\ V_{SHE}$). Therefore, if NP Cu is immersed in a solution containing $PtCl_4^{2-}$, the spontaneous reaction will proceed as follows: $2Cu + PtCl_4^{2-} \rightarrow Pt + 2\ Cu^{2+} + 4Cl^-$. Oxidation of Cu before galvanic displacement poses a severe limitation to catalyst production, so care was taken to reduce all NP Cu for 2 hours at 450 °C in an H_2 stream prior to displacement. Figure 2 offers proof of concept that the novel method of drop-casting NP Cu precursor onto a GC disk electrode, followed by an 'in-situ' galvanic displacement using the RDE is possible. The reddish tint of copper in Figure 2a is replaced by the grey tint of Pt particles (Figure 2b) after immersing

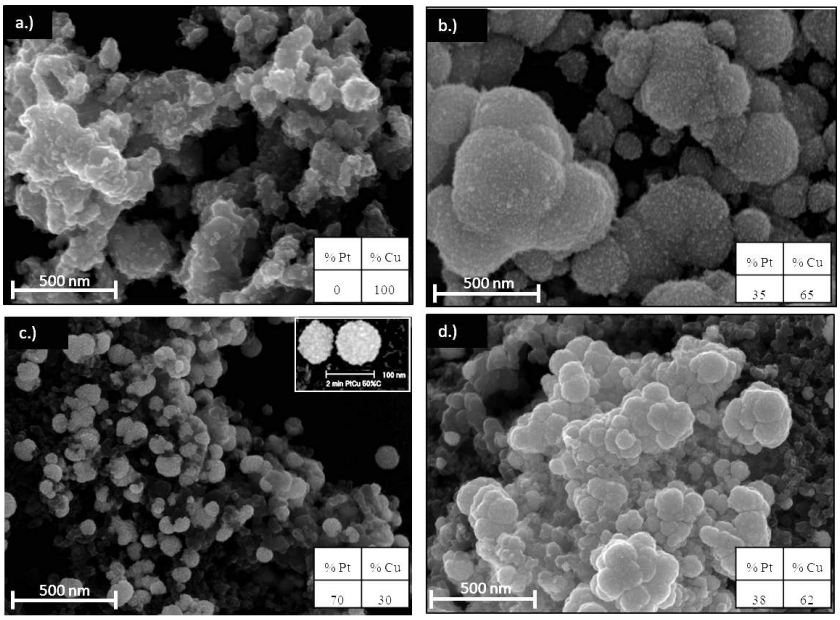

Figure 3. SEM images of a.) NP Cu before displacement, b.) PtCu after 2min RT displacement, c.) PtCu/C after 2 min 50 deg displacement, and d.) PtCu/C after 2 min 50 °C displacement in 0.12 mM K_2PtCl_4. Insets show atomic % of Pt and Cu derived from EDX analysis ([K_2PtCl_4] = 1.2 mM unless noted otherwise)

the entire disk assembly in a solution of 1.2 mM K_2PtCl_4. It is important to note that the Pt ring electrode was not altered during the reaction; the galvanic displacement process is selective to copper.

An array of PtCu catalysts were prepared by 1) modifying the time and/or temperature of galvanic displacement, or 2) modifying the concentration of K_2PtCl_4 used during displacement. Time of deposition varied between 2-5 minutes, while temperature during deposition varied from 5 °C to 60 °C. Concentration of K_2PtCl_4 was either 0.12 mM or 1.2 mM. Several catalysts were also prepared with a 50 wt% Vulcan XC 72 carbon support (referred to as PtCu/C). The effect of temperature and [K_2PtCl_4] on the resulting catalyst morphologies/compositions is shown in Figure 3. It should be noted that the morphology of NP Cu changes dramatically after it undergoes the sonication process involved with drop casting it onto the GC electrode. After two minutes of galvanic displacement at RT (Figure 3b) the profile of the NP Cu changes dramatically—by this time, it appears that Pt has completely filled the smaller pores.

Interestingly, the EDX composition does not indicate that there is an excess of Pt—the composition is 65% Cu. This suggests the presence of a core-shell structure with a Pt-rich shell and a Cu-rich core. Upon increasing the temperature during galvanic displacement to 50 °C (Figure 3c), two interesting things happen— 1) PtCu core-shell particles with about 80 nm diameters appear on the surface of the electrode, and 2) the Pt composition increases to 70%. Other SEM images of the catalysts (taken at lower magnification) always show some void space on the PtCu coated electrode; however, all catalysts coated at 50 °C have substantially lower void space due to the growth of the PtCu particles. This is quite unexpected, and currently we have no absolute explanation for why it happens. As a control experiment, a 2 min 50 °C galvanic displacement was performed on a 'blank' Vulcan XC-72 coated electrode. As expected, there was no growth of the small particles, nor was there any evidence of Pt from EDX analysis. If the concentration of K_2PtCl_4 during displacement is decreased tenfold (Figure 3d), the reaction occurs slower (rate $\propto [PtCl_4^-]$). Therefore, after 2 min, the Pt composition is 60% lower, relative to the same displacement with a high K_2PtCl_4 concentration. Increasing the time of displacement past 2 mins does not seem to increase the incorporation of Pt much past 70%. This would suggest that as more Pt is incorporated into the NP Cu structure, the reduction potential for the PtCu surface increases to a point where there is no longer a thermodynamic driving force for galvanic displacement. These results are in good agreement with galvanic displacement findings from Mohl et al.[45]

As prepared, the PtCu catalysts still had areas of exposed Cu, and the CVs were not immediately at steady state. As a result, all catalysts were electrochemically cycled in N_2 saturated electrolyte (as described in Experimental section) until a stable CV was obtained. This extra step is very similar to 'dealloying' described by Koh et al.,[43] but slightly different because

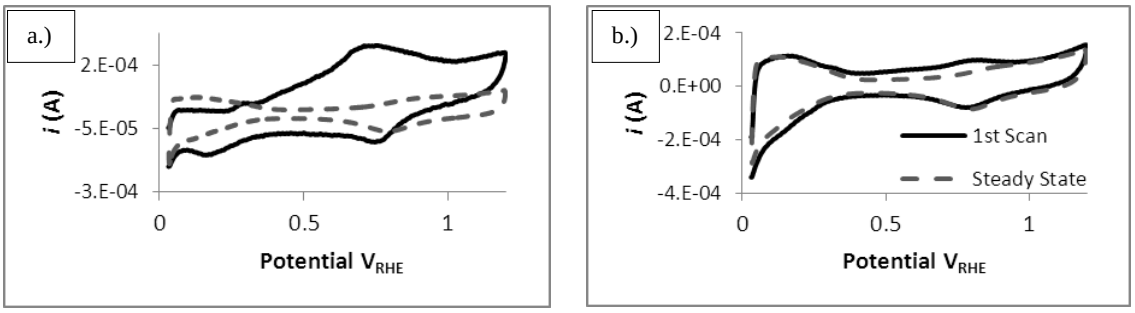

Figure 4. Effect of dealloying. 1st CV compared to steady state CV for a.) 2 min RT PtCu, and b.) 3 min 50 deg PtCu. N_2 saturated 0.1 M $HClO_4$; 100 mV/s.

the catalysts already have a Pt-rich shell from galvanic displacement. The effects of dealloying scale with the extent of galvanic displacement. For catalysts displaced at lower temperatures and lower K_2PtCl_4 concentrations, dealloying had a pronounced effect. In Figure 4a the 1st CV shows a large wave of Cu dissolution in the anodic scan. For catalysts displaced at higher temperatures and higher K_2PtCl_4 concentrations, there was almost no effect from dealloying (Figure 4b; little deviation between 1st CV and steady state CV).

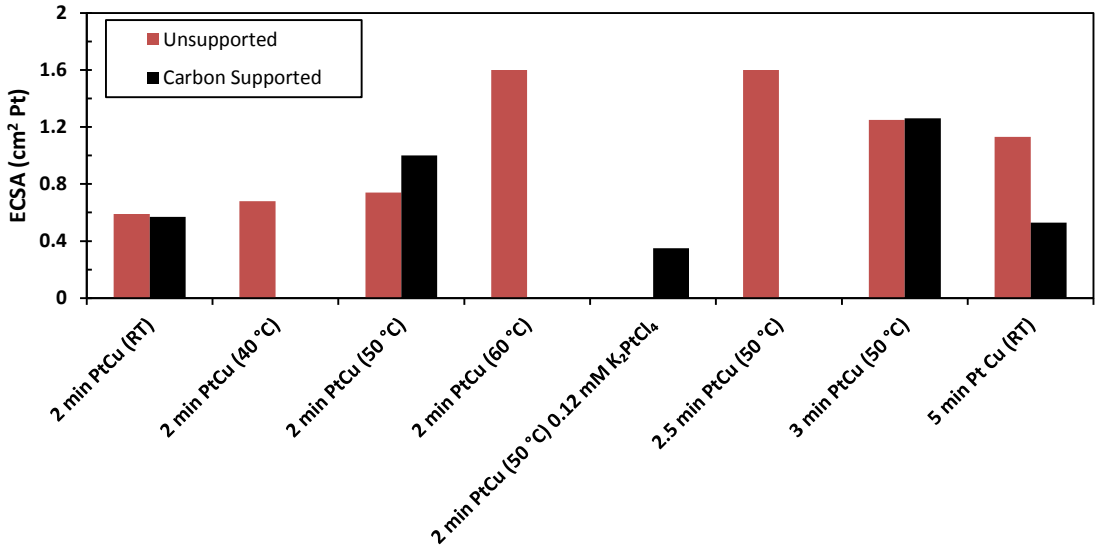

Figure 5. Pt ECSA for catalysts. Determined using H_{upd} from steady state CVs obtained in N_2 saturated $HClO_4$

Pt ECSA was determined from the charge passed during H_{upd} as described in the Experimental section. Figure 5 shows the resulting Pt ECSAs for the array of PtCu catalysts. The highest Pt ECSAs are observed for the 2 min 60 °C catalyst and the 2.5 min 50 °C catalyst. The

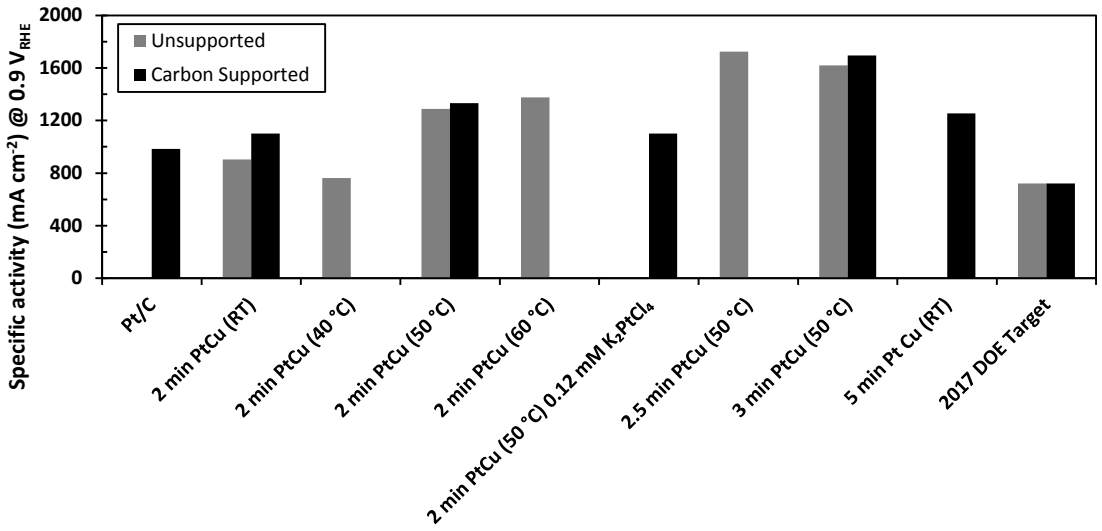

Figure 6. ORR activity normalized to total Pt ECA compared to Pt/C and DOE 2017 target. Activities were measured at 0.9 V_{RHE} during anodic polarization sweeps at 298K, 1600 RPM and 100 mV s^{-1} in O_2 saturated 0.1 M $HClO_4$

general trend follows logically—as the time/temperature during displacement increases, the Pt ECSA increases. Pt ECSA reaches a maximum with the 2 min 60 °C catalyst. The second highest Pt ECSA belongs to the 2.5 min 50 °C catalyst, rather than the more logical 3 min 50 °C catalyst. This unexpected result can be explained by considering that the Pt ECSA has a volcano-like dependency on time of displacement. After a period of time, here 2.5 minutes, the ECSA begins to decrease. From this, it could be hypothesized that the surface area of the PtCu catalyst will decrease if the galvanic displacement occurs for too long. Although this may increase the specific activity (activity per Pt ECSA) of catalysts displaced for time periods > 2.5 minutes, it would be detrimental to the mass activity (activity per g Pt), which is a more important activity metric.

Mass transfer corrected ORR activities of PtCu catalysts at 0.9 V were normalized to Pt ECSAs and compared to the current state-of-the-art commercially available Pt catalyst (denoted as 'Pt/C') in Figure 6. For the most part, the PtCu catalysts outperform the Pt/C standard. The optimal catalyst shown here is the 2.5 min 50 °C catalyst. It outperforms Pt/C by a factor of 1.75. The 2017 DOE target for ORR specific activity (SA) is 720 µA cm^{-2}; the 2.5 min 50° C PtCu

catalyst exceeds that target by more than twofold. It is worth noting that supporting the PtCu catalysts on C does not seem to affect the SAs of the catalysts, despite the fact that there is 50% less Cu in the initial catalyst. In addition, there is no negative correlation between ECSA and SA, which reinforces the validity of the data. Mass transfer corrected Tafel plots are shown in Figure 7 to compare the activity of the catalysts between 0.85 V and 1.0 V. From Figure 7, it is clear that PtCu offers a considerable activity improvement over the Pt/C standard. The slope of the Tafel plots is very close to 60 mV/dec for all of the catalysts, indicating the rate determining step for ORR is not an electron transfer step, but most likely the cleavage of the O_2 bond.

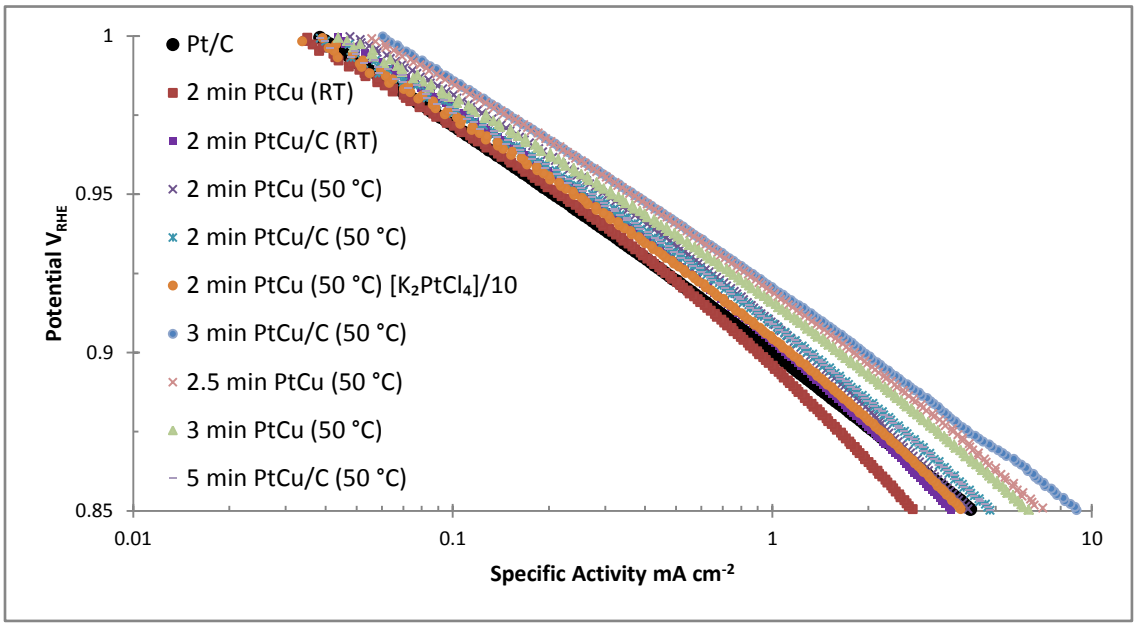

Figure 7. Tafel plots for the ORR using anodic polarization sweeps at 298 K, 1600 RPM and 100 mV s^{-1} in O_2-saturated 0.1 M $HClO_4$

The conclusion that our PtCu catalysts are superior ORR catalysts to Pt/C is true even when the mass activities at 0.9 V are compared. Table 1 compares the mass activity (MA) of several PtCu catalysts to Pt/C. The 3 min 50 °C PtCu catalyst compares well, with a MA advantage 1.4 times that of Pt/C. The 2 min RT PtCu catalyst also performs quite well in the MA category, but it has a mediocre specific activity. We think this is the result of the catalyst not

Table 1. Summary of mass activity and stability for PtCu catalysts

Catalyst	Mass Activity ($A\ mg\ Pt^{-1}$)	Specific Activity ($\mu A\ cm^{-2}$)	% loss after 10,000 cycles 0.6 - 1.1 V_{RHE}
2 min PtCu (RT Galv. Disp.)	0.245	991	------
3 min PtCu/C (50 °C Galv. Disp.)	0.253	1695	**0% activity loss** 19.3% loss in ECSA after 5,000 cycles. 0 % loss in ECSA between 5,000 - 10,000 cycles.
5 min PtCu	0.100	681	------
Pt Black/C	0.178	984	------
2017 DOE Target (80 °C)	≥0.44	720	< 40%

being displaced with enough Pt to experience the catalytic benefit enjoyed by the other, more well displaced catalysts. The 5 min RT PtCu catalyst has a low MA because it has a substantially lower surface area. The key to improving the MA of our catalysts is to increase their surface area. It is evident from the SEM images in Figure 3 that the Pt is not forming an even coating on the NP Cu. Pt that is not at the surface cannot participate in the ORR, so it is essentially wasted Pt. We suspect that although we have reasonable MA, we could have significantly higher MA if we can form a thinner and more uniform catalyst coating. Nevertheless, our catalysts experience a real enhancement relative to Pt/C, and we attribute this enhancement to the core-shell structure they obtain during galvanic displacement and subsequent dealloying.

Stability and durablity will always be a concern for ORR catalysts. To measure the stability of our catalysts we used a modification of the accelerated stability test used by Kibsgaard et al.[46] The test was performed by cycling the potential between 0.6 and 1.1 V_{RHE} in O_2 saturated 0.1 M $HClO_4$ for 10,000 cycles. Each 5000 cycles the electrolyte was saturated with nitrogen and the ECSA measured. The results of this test are shown in Table 1. The 3 min 50 °C

PtCu catalyst experienced 0% loss in activity over the 10,000 cycles. The ECSA decreased by 20% during the first 5000 cycles, but remained constant during the subsequent 5000 cycles. Interestingly, the raw ORR currents obtained for cycle 1 and cycle 10,000 were the same, indicating that the specific activity of the catalyst increased over the 10,000 cycles.

4. Conclusions

We used a novel method of performing the galvanic displacement reaction to produce several core-shell PtCu catalysts from nanoporous copper and K_2PtCl_4 precursors. We investigated the oxygen reduction kinetics of several of these PtCu catalysts and found them to have specific and mass activities superior to the current state-of-the-art Pt/C catalyst. The 3 min 50 °C catalyst was found to have no activity losses over 10,000 potential cycles. Despite the superior activity, we are not convinced that this method cannot be tuned further to produce even more active catalysts. Initially, we believed that the thinner our Pt layer, the more enhancement in ORR we would see, and while this is true for specific activity, the raw currents for such a catalyst would be painfully low. It would require a substantial amount of catalyst to drive the ORR at an appreciable rate. In a real fuel cell system, mass transport becomes an issue as the catalyst loading increases. From this work, we believe that there may be some inherent catalytic advantage to galvanic displacement of Cu with Pt, particlarly at the higher temperatures where the catalyst particles seem to spawn from the glassy carbon. It would also be interesting to translate this galvanic displacement method to another system like nanoporous cobalt, as cobalt alone enjoys a higher inherent ORR activity than Cu.

Acknowledgements

This work was supported and funded by The Ohio State University. I would also like to thank Sarum Boonmee for preparing our Cu-Al alloys. I also gratefully acknowledge the Ohio State

University Graduate Enrichment Fellowship.

References

1. Vielstich, W.; Gasteiger, H. A.; Lamm, A.; Yokokawa, H., *Handbook of Fuel Cells: Fundamentals, Technology, and Applications*. 2003; Vol. 3.
2. Service, R. F., *Science* **2004,** *305* (5686), 958-961.
3. Mayrhofer, K. J. J.; Strmcnik, D.; Blizanac, B. B.; Stamenkovic, V.; Arenz, M.; Markovic, N. M., *Electrochimica Acta* **2008,** *53* (7), 3181-3188.
4. Stamenkovic, V.; Mun, B. S.; Mayrhofer, K. J. J.; Ross, P. N.; Markovic, N. M.; Rossmeisl, J.; Greeley, J.; Nørskov, J. K., *Angewandte Chemie International Edition* **2006,** *45* (18), 2897-2901.
5. Stamenkovic, V. R.; Mun, B. S.; Arenz, M.; Mayrhofer, K. J. J.; Lucas, C. A.; Wang, G.; Ross, P. N.; Markovic, N. M., *Nat Mater* **2007,** *6* (3), 241-247.
6. Makharia, R.; Kocha, S.; Yu, P.; Sweikart, M. A.; Gu, W.; Wagner, F.; Gasteiger, H. A., *ECS Transactions* **2006,** *1* (8), 3-18.
7. Wagner, F. T.; Gasteiger, H. A.; Makharia, R.; Neyerlin, K. C.; Thompson, E. L.; Yan, S. G., *ECS Transactions* **2006,** *3* (1), 19-29.
8. Toda, T.; Igarashi, H.; Watanabe, M., *Journal of Electroanalytical Chemistry* **1999,** *460* (1–2), 258-262.
9. Wang, J. X.; Inada, H.; Wu, L.; Zhu, Y.; Choi, Y.; Liu, P.; Zhou, W.-P.; Adzic, R. R., *Journal of the American Chemical Society* **2009,** *131* (47), 17298-17302.
10. Stamenkovic, V. R.; Fowler, B.; Mun, B. S.; Wang, G.; Ross, P. N.; Lucas, C. A.; Marković, N. M., *Science* **2007,** *315* (5811), 493-497.
11. Bing, Y.; Liu, H.; Zhang, L.; Ghosh, D.; Zhang, J., *Chemical Society Reviews* **2010,** *39* (6), 2184-2202.
12. Henry, J. B.; Maljusch, A.; Huang, M.; Schuhmann, W.; Bondarenko, A. S., *ACS Catalysis* **2012,** *2* (7), 1457-1460.
13. Paulus, U. A.; Wokaun, A.; Scherer, G. G.; Schmidt, T. J.; Stamenkovic, V.; Radmilovic, V.; Markovic, N. M.; Ross, P. N., *The Journal of Physical Chemistry B* **2002,** *106* (16), 4181-4191.
14. van der Vliet, D.; Wang, C.; Debe, M.; Atanasoski, R.; Markovic, N. M.; Stamenkovic, V. R., *Electrochimica Acta* **2011,** *56* (24), 8695-8699.
15. Marković, N. M.; Schmidt, T. J.; Stamenković, V.; Ross, P. N., *Fuel Cells* **2001,** *1* (2), 105-116.
16. Sarkar, A.; Manthiram, A., *The Journal of Physical Chemistry C* **2010,** *114* (10), 4725-4732.
17. Sun, Z.; Masa, J.; Xia, W.; König, D.; Ludwig, A.; Li, Z.-A.; Farle, M.; Schuhmann, W.; Muhler, M., *ACS Catalysis* **2012,** *2* (8), 1647-1653.
18. Wang, C.; Markovic, N. M.; Stamenkovic, V. R., *ACS Catalysis* **2012,** *2* (5), 891-898.
19. Strasser, P.; Koh, S.; Yu, C., *ECS Transactions* **2007,** *11* (1), 167-180.
20. Stephens, I. E. L.; Bondarenko, A. S.; Gronbjerg, U.; Rossmeisl, J.; Chorkendorff, I., *Energy & Environmental Science* **2012,** *5* (5), 6744-6762.
21. Kinoshita, K., *Journal of The Electrochemical Society* **1990,** *137* (3), 845-848.
22. Strasser, P.; Koh, S.; Anniyev, T.; Greeley, J.; More, K.; Yu, C.; Liu, Z.; Kaya, S.; Nordlund, D.; Ogasawara, H.; Toney, M. F.; Nilsson, A., *Nat Chem* **2010,** *2* (6), 454-460.

23. Neergat, M.; Rahul, R., *Journal of The Electrochemical Society* **2012,** *159* (7), F234-F241.
24. Yang, H.; Alonso-Vante, N.; Léger, J.-M.; Lamy, C., *The Journal of Physical Chemistry B* **2004,** *108* (6), 1938-1947.
25. Beard, B. C.; Ross, P. N., *Journal of The Electrochemical Society* **1990,** *137* (11), 3368-3374.
26. Qian, Y.; Wen; Adcock, P. A.; Jiang, Z.; Hakim, N.; Saha, M. S.; Mukerjee, S., *The Journal of Physical Chemistry C* **2008,** *112* (4), 1146-1157.
27. Soderberg, J. N.; Sirk, A. H. C.; Campbell, S. A.; Birss, V. I., *Journal of The Electrochemical Society* **2005,** *152* (10), A2017-A2022.
28. Lima, F. H. B.; de Castro, J. F. R.; Santos, L. G. R. A.; Ticianelli, E. A., *Journal of Power Sources* **2009,** *190* (2), 293-300.
29. Yang, R.; Leisch, J.; Strasser, P.; Toney, M. F., *Chemistry of Materials* **2010,** *22* (16), 4712-4720.
30. Chen, H. M.; Liu, R.-S.; Lo, M.-Y.; Chang, S.-C.; Tsai, L.-D.; Peng, Y.-M.; Lee, J.-F., *The Journal of Physical Chemistry C* **2008,** *112* (20), 7522-7526.
31. Hou, L.; Qiu, H., *Journal of Power Sources* **2012,** *216* (0), 28-32.
32. Zhou, X.; Gan, Y.; Du, J.; Tian, D.; Zhang, R.; Yang, C.; Dai, Z., *Journal of Power Sources* **2013,** *232* (0), 310-322.
33. Shao, M.; Shoemaker, K.; Peles, A.; Kaneko, K.; Protsailo, L., *Journal of the American Chemical Society* **2010,** *132* (27), 9253-9255.
34. Mathew, P.; Meyers, J. P.; Srivastava, R.; Strasser, P., *Journal of The Electrochemical Society* **2012,** *159* (5), B554-B563.
35. Oezaslan, M.; Hasché, F.; Strasser, P., *Journal of The Electrochemical Society* **2012,** *159* (4), B444-B454.
36. Oezaslan, M.; Hasché, F.; Strasser, P., *Journal of The Electrochemical Society* **2012,** *159* (4), B394-B405.
37. Zhang, X.; Wang, H.; Key, J.; Linkov, V.; Ji, S.; Wang, X.; Lei, Z.; Wang, R., *Journal of The Electrochemical Society* **2012,** *159* (3), B270-B276.
38. Cochell, T.; Manthiram, A., *Langmuir* **2011,** *28* (2), 1579-1587.
39. Wu, J.; Peng, Z.; Yang, H., *Philosophical Transactions of the Royal Society A: Mathematical, Physical and Engineering Sciences* **2010,** *368* (1927), 4261-4274.
40. Xu, C.; Liu, Y.; Wang, J.; Geng, H.; Qiu, H., *ACS Applied Materials & Interfaces* **2011,** *3* (12), 4626-4632.
41. Alia, S. M.; Jensen, K. O.; Pivovar, B. S.; Yan, Y., *ACS Catalysis* **2012,** *2* (5), 858-863.
42. Kristian, N.; Yu, Y.; Lee, J.-M.; Liu, X.; Wang, X., *Electrochimica Acta* **2010,** *56* (2), 1000-1007.
43. Koh, S.; Strasser, P., *Journal of the American Chemical Society* **2007,** *129* (42), 12624-12625.
44. Gasteiger, H. A.; Kocha, S. S.; Sompalli, B.; Wagner, F. T., *Applied Catalysis B: Environmental* **2005,** *56* (1–2), 9-35.
45. Mohl, M.; Dobo, D.; Kukovecz, A.; Konya, Z.; Kordas, K.; Wei, J.; Vajtai, R.; Ajayan, P. M., *The Journal of Physical Chemistry C* **2011,** *115* (19), 9403-9409.
46. Kibsgaard, J.; Gorlin, Y.; Chen, Z.; Jaramillo, T. F., *Journal of the American Chemical Society* **2012,** *134* (18), 7758-7765.